Fuć, PAWEŁ **PTNSS–2011–SC–134**

The initiation of Diesel Particulate Filter regeneration via thermoelectric generator

Abstract: One of the main limitations in diesel engine applications is the emission of particulate matter. This problem has been solved by the application of diesel particulate filters also referred to as DPF. This solution unfortunately turned out to be far from perfect. The main problems of DPFs are their regeneration (burning of soot accumulated in the filter) and their durability. Such a situation resulted in a need to launch research that aims at more efficient solutions.

In the paper the author discusses the possibility of DPF regeneration through the use of catalytic support material at the same time being an ionic conductor. Ti_4O_7 has been used as the base material. The paper presents the basic parameters of the described material. Besides, basic test of the system of exhaust gas recuperation has been presented that could potentially generates energy needed for the initiation of the filter regeneration process in order to secure a continuous soot afterburning process.

Key words: *diesel particulate filter, exhaust gas recuperation*

Inicjacja filtra cząstek stałych przez generator termoelektryczny

Streszczenie: Jednym z głównych ograniczeń stosowania silników o zapłonie samoczynnym jest emisja cząstek stałych. Problem ten rozwiązano przez zastosowanie filtra cząstek stałych (DPF). Jednak rozwiązanie to okazało się dalece niedopracowane. Głównymi problemami są regeneracja filtra, czyli wypalanie sadzy zgromadzonej w filtrze oraz trwałość. To spowodowało konieczność prowadzenia badań mających na celu opracowanie skuteczniejszych konstrukcji.

W pracy rozważaniu poddano możliwość regeneracji filtra cząstek stałych przy zastosowaniu materiału nośnika będący przewodnikiem jonowym. Jako materiał bazowy użyto Ti_4O_7. Zaprezentowano podstawowe parametry opisywanego materiału. Ponadto przedstawiono badania podstawowe układu rekuperacji spalin stanowiącego potencjalną możliwość generowania energii umożliwiającej zapoczątkowanie procesu regeneracji w celu zapewnienia ciągłego procesu wypalania sadzy.

Słowa kluczowe: *filtr cząstek stałych, rekuperacja spalin*

1. Introduction

The principle of operation of PM emission reduction systems differs depending on the applied concept but the most frequently used are CRT – continuous regeneration trap, CSF – catalyst soot filter, CCRT – catalyst continuous regeneration trap and DPNR – diesel particulate NOx reduction (fig. 1, 2). An important role in these systems play catalytic layers. It is because of their presence that the reaction of afterburning of soot with the help of NO_2 or O_2 is possible. Depending on the method of achieving the temperature of the catalytic reaction in the filter we can distinguish a passive and active regeneration [3], [8].

A basic factor needed for the occurrence of passive regeneration with a sufficient efficiency is an appropriate temperature of the exhaust gases that, depending on the system, must exceed 280–350^{o}C as well as an even temperature distribution in the diesel particulate filter support. Another important factor is the lowest possible ratio of NOx/PM [13].

Active regeneration defined as a method of soot removal that gathers on the filter through supplying additional energy to the exhaust system is done by oxidizing the soot (soot afterburning) by NO_2 or O_2 [4], [5]. If the emission of NOx from the engine is sufficient, the oxidation of soot can be done with NO_2. The required temperature is 300–350^{o}C. If the engine operates at parameters that do not ensure such a temperature it can be reached by an additional injection of fuel into the exhaust system or the cylinder in the exhaust stroke. Regeneration through oxidation of soot with NO_2 requires more time (due to an insufficient concentration of NOx in the exhaust gases) but is much safer in terms of the filter durability. If the emission of NOx from the engine is insufficient then active regeneration (oxidation C) can be done with O_2 but an increase in the temperature is necessary in the filter to 550–600^{o}C. Such a temperature is obtained through an additional fuel injection by an additional injector into the cylinder in the exhaust stroke or directly into the exhaust system.

An alternative for obtaining of an appropriate temperature necessary for a successful regeneration of the diesel particulate filter, passive regeneration in particular is the possibility of use of a composite material used for the construction of the filter. This

will allow obtaining an appropriate temperature using the electron conductivity of one of the layers.

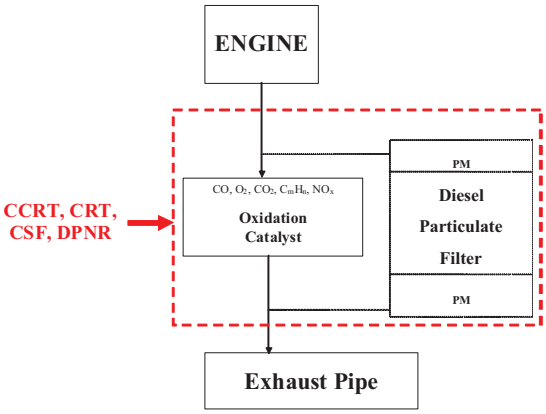

Fig. 1. A schematic diagram of exhaust aftertreatment systems used in combustion engines

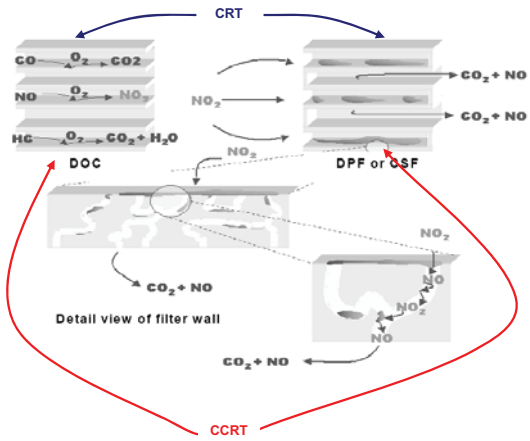

Fig. 2. Schematics of the diesel particulate filter regeneration and PM emission reduction systems currently available in the market: CRT, CSF, CCRT

Modern vehicles are fitted with a variety of electronically controlled subcomponents related to the engine operation and other vehicle elements that require much energy. At the same time we have been aware for years that one of the main combustion energy losses are thermal losses in the exhaust systems. The technology aiming at the recuperation of this energy is continuously improved. It is a real alternative for obtaining of part of the energy needed for the diesel particulate filter regeneration assuming a specific filter support design [12].

Recent years have seen many papers devoted to the regeneration of diesel particulate filters [6], [7], [9], [14]. To date it has been a very up-to date issue and the above-described systems need constant development. Each of these systems requires a different improvement in design. There is however a common factor that decides about the efficiency of the filter the fracture effect that substantially influences the efficiency of the filtration and filter regeneration [10].

2. The tests on the ionic conductor as a material for the construction of the diesel particulate filter

2.1. The construction of the filter support from a highly porous z Ti_4O_7

The support in the diesel particulate filter, in order to generate a turbulent exhaust flow, needs to be composed of three types of pores. Open pores should be of the size from several μm to several mm, mesopores half open should be of the size of several μm and the walls of these pores built from micropores should be of the size below 1 μm. Both the mesopores and micropores are located in the walls of the macropores. Such ceramic sinters are made through sintering of micro grains of Ti_4O_7, introduced to the sponge-like model structures, made from a polymer. In the past a methodology was developed of obtaining the nanospheres of TiO_2 through FSP (flame spray pyrolysis) that were subjected to a thermal processing and then heating in hydrogen in order to obtain Ti_4O_7 (fig. 3). Such a paste was mixed with the organic gel Tixo 221 by HERAEUS. Through a multiple process of paste introduction (the gel and the Ti_4O_7 nanograins) a deep penetration of the grains of Ti_4O_7 was obtained in a microporous polymer sponge. Such a support of the DPF filter was dried in a vacuum dryer [1], [2], [11].

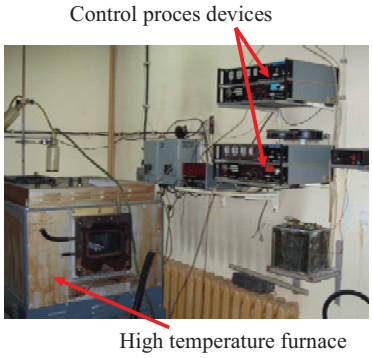

Fig. 3. Device for heating of the samples in hydrogen

In this way the filter support with four types of pores was obtained – closed and open Macropores of the diameter of 200–400 nm, closed and open mesopores of the diameter of 50–100 μm and the micropores of the diameter below 1 μm. The advantage of the support built from Ti_4O_7 as compared to a classic SiC support is the microporous structure that enables anchoring of the catalysts on the surfaces of open and half open micro- and mesopores without the necessity to perform an additional surface processing – etching and intermediate layer application.

Figure 4 presents the image of the catalytic support, whose total porosity was 63%.

a)

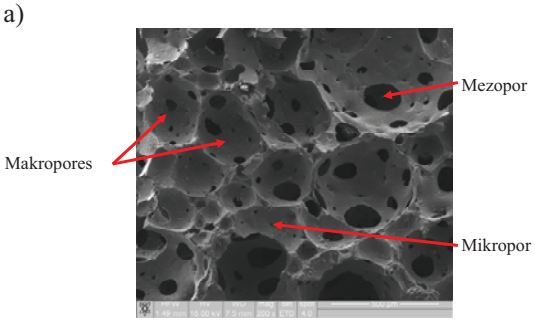

b)

Fig. 4. The view of the Ti_4O_7 of the porosity of 63%: a) enhanced image with the macro-, meso- and micropores marked; b) the support was covered with Ti_4O_7 with the use of SiC support as the prime layer

The presented material is also an ionic conductor which is the basis for the initiation of the soot afterburning reaction with electric current, whose one of the sources could be the exhaust gas energy recuperator.

2.3. Measurements of the thermal properties of Ti_4O_7 with the laser flash method

2.3.1. The characteristics of the research method

Thermal conductivity λ, diffusivity α and specific heat c_p were measured with laser-flash method (LFA 457 MicroFlash by Netzsch) in the Thermoelectric Laboratory at the Faculty of Material Engineering and Ceramics, University of Science and Technology in Cracow (tab. 1).

The Laser Flash method enables a direct measurement of the thermal diffusivity of solid bodies in the form of solid pellets, layers, powders and liquids. The advantages of this method are high accuracy, repeatability of the obtained results, quick measurement time, simple preparation of samples and non-destructive nature of the tests.

In the laser flash method one of the surfaces of the samples is heated with a short flash of laser radiations. At the same time the growth in the temperature is recorded on the opposite sample through an IR detector. Based on dependence T'(t) a coefficient of thermal diffusivity α is determined. Specific heat of the tested material c_p is determined through comparing of the temperature change of the tested sample ΔT_p with the change of the temperature of the reference specimen ΔT_w. Based on the measured parameters α, c_p and density of the material ρ we can determine its thermal conductivity λ.

Table 1
Technical specifications- LFA 457 Netzsch

Temperature range	-125 °C to 1100 °C
Laser type Nd-YAG	Energy: from 0 J to 18.5 J, impulse width: 0.5 ms
Types of sensors	MCT (Mercury Cadmium Telluride), InSb (Indium Antimonide), cooled with liquid nitrogen
Thermal diffusivity range	1 mm^2/s to 1000 mm^2/s
Thermal conductivity range	0.1 W/(m·K) to 2000 W/(m·K)
Repeatability of the measurement results of thermal diffusivity	±2% (for standard materials)
Repeatability of the measurement results of specific heat	±3% (for standard materials)
Accuracy of the measurements of thermal diffusivity	±3% (for most of the materials)
Accuracy of the measurements of the specific heat	±5% (for most of the materials)

$$\lambda(T) = \rho(T)\cdot c_p(T)\cdot\alpha(T) \qquad (1)$$

The laser-flash method allows determining of the thermal parameters of the tested samples in the temperature range from -125°C to 1100°C with the accuracy of 5% for a wide variety of materials (tab. 1).

2.3.2. Results

The tests of the properties of Ti_4O_7 were performed on samples of diameter of 10 mm and thickness of 2,9 mm. The determined density of the samples was $\rho = 2.17\ g/cm^3$. The samples were covered with a layer of graphite in order to maintain appropriate conditions of absorption and emission of heat. The measurements were performed at the following parameters: voltage V = 1.8 kV, laser flash duration t = 5 ms, in nitrogen N_2 with the flow rate $v = 20cm^3/h$ in the temperature range of 25–600°C. The specific heat was determined with the comparative method (graphite reference sample of the diameter of 10 mm and thickness of 1.2 mm). Figure 5 presents the example results for a single measurement performed in the temperature of 100°C.

The experimental kinetic curves have been described with a high level of accuracy with the Cappe-Lehman model that takes into account the adjustment of duration of the flash. Figures 6 and 7 present the values of thermal diffusivity calculated for different temperatures α and the Ti_4O_7 temperature dependence of specific heat c_p.

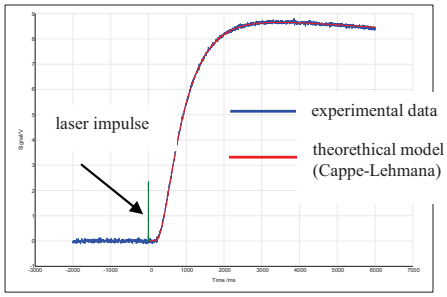

Fig. 5. Signal from the InSb sensor for the Ti_4O_7 sample measured in the temperature of 100°C

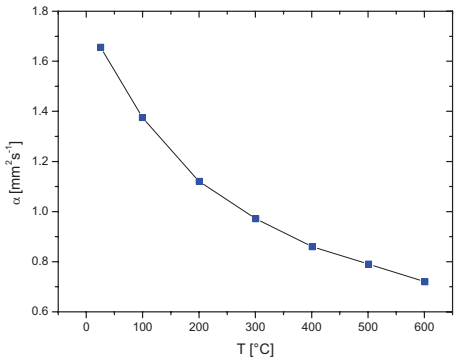

Fig. 6. Thermal diffusivity of the Ti_4O_7 sample as a function of laser flash

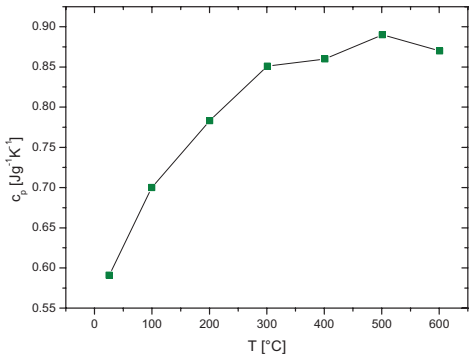

Fig. 7. Specific heat of the Ti_4O_7 sample as a function of temperature

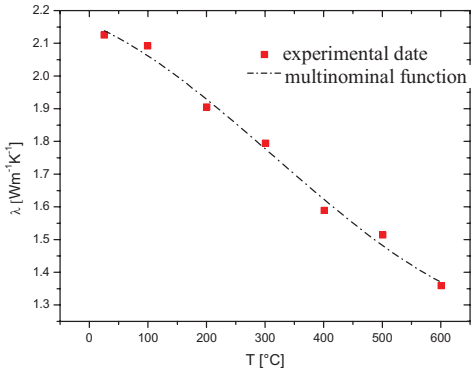

Fig. 8. Thermal conductivity of the Ti_4O_7 sample as a function of temperature

Based on the obtained results of the measurements of specific heat c_p, thermal diffusivity α and density ρ the thermal conductivity of material λ (fig. 8) was obtained from formula (1).

3. Preliminary investigations into the thermoelectric generator

3.1. Tests on the engine test bed

The tests were performed using the self-ignition engine of 1.3 dm^3 displacement, with the direct common-rail injection and the Automex eddy-current brake dynamometer (tab. 2). The engine was controlled by a modified electronic system. The preliminary measurements of the heat exchange mounted on the exhaust system of the engine were conducted on the engine test bed. The tests were performed for the engine parameters including the operating range used in the real operation in road conditions. The authors selected the parameters based on their own experience. To give the full picture of the operating conditions of the generator the measurements were taken in the full load characteristics at selected engine speeds, allowing the operation of the heat exchanger in the broad loading range (20-120 Nm).

Table 2

Engine and brake specification

Engine specification	
Capacity	1.3 dm^3
Engine power	51 kW / 4000 rpm
Torque	180 Nm / 1750 rpm
Cylinders	4
Valves	16
Injection system	common rail
Brake specification	
Type	AMX – 210/100
Maximum power	100 kW
Maximum torque	240 Nm
Maximum rpm	10000 rpm

The research included:

- the measurement of temperatures in the twelve points along the whole length of the heat exchange, on the upper and lower cooler contact surface with the heat exchanger (fig. 9, 10),
- measurement of the coolant flow through the coolers,
- measurement of the exhaust gas temperatures in front and behind the heat exchanger,
- measurement of fuel consumption,
- measurement of air consumption,
- measurement of received power by the water flowing through the coolers contacting the upper and lower surface of the exchanger.

Two variants of heat exchangers were tested. The difference between them was related to the modification of the inlet and outlet cone. The first variant caused the exhaust gases to cool down in the first stage of the flow through the recuperator,

which resulted in lowering the temperature in the second part of the recuperator. The test results presented are for variant two with the improved exhaust gas flow conditions.

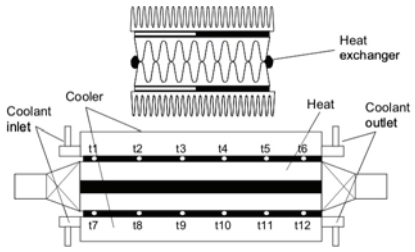

Fig. 9. Cross-section of the thermoelectric generator

Fig. 10. Picture of the thermoelectric generator mounted on exhaust system of self-ignition engine

In order to compare the temperature distribution on the upper and lower cooler the temperatures were measured at 2300 rpm and 20-120 Nm load. Also the temperature distribution on the lower cooler was presented at engine speeds of 1700 and 3300 rpm. Also the power received from the exhaust system was compared; the power received by the agent flowing through the cooler was calculated.

3.2. Results

The distribution of temperatures between the upper and lower cooler and the exchanger differs both in the temperature level and distribution in the particular measurement points (Fig. 11). The distribution of temperatures in the lower cooler is more uniform, which means the flow of exhaust gases, or rather the heat absorption by the lower part of the heat exchange is more efficient as compared to the upper part. It is most probably due to the less turbulent flow of the exhaust gases in the lower part of the exchanger.

The testing of the temperature distribution was performed at different engine speeds: 2300, 3300 rpm. The temperatures received at lower engine speed are higher, even though the difference of temperature of the exhaust gases measured for the both engine speeds in front of and behind the recuperator is at every engine load point higher for the 3300 rpm by 50°C on average. However, in the first case the coolant flow of 21 l/h was used.

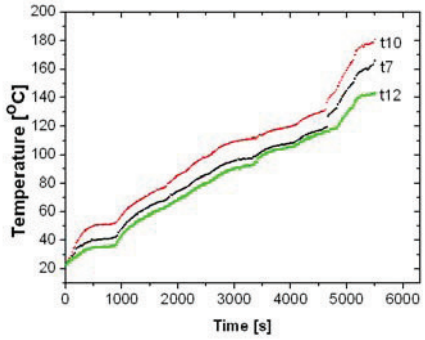

Fig. 11. Temperature from the cooled side of the heat exchanger [13]

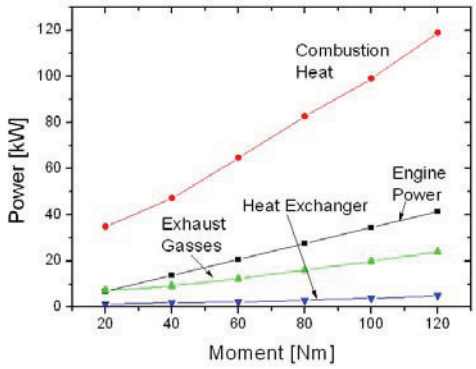

Fig. 12. Generated and recuperated heat comparison at engine speed 3300 rpm and different load [13]

At 3300 rpm the flow was 10 times higher, which lead to smaller differences in coolant temperature in front of and behind the coolers, and at the same time to the greater efficiency of heat absorption from exhaust gases. This situation is illustrated by Fig. 12, which shows that the most efficient operation of the system was at 3300 rpm. The recuperator built enabled the maximum recuperation of 4.2 kW at fuel consumption of 4.6 kg, air consumption of 87 kg/h and the resulting combustion heat of 118 kW at engine power of 42 kW (engine speed of 3300 rpm and 120 Nm load) (fig. 13).

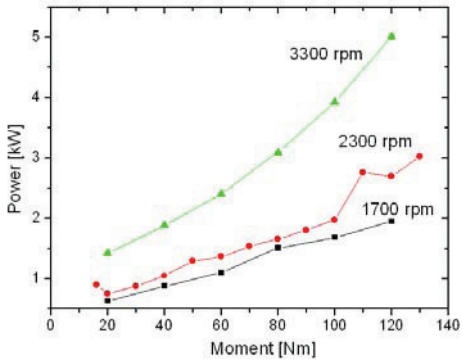

Fig. 13. Recuperated power with different engine speed and load

4. Conclusions

Research has been done consisting in modification of the SiC catalytic supports currently in use in the aftertreatment systems and diesel particulate filters. Nanopowders have been obtained for research aiming at their introduction in the design of catalytic supports, washcoats or active catalytic layers. A prototype of a new catalytic support has been developed that uses Ti_4O_7 nanospheres formed through a flame spray pyrolysis that after an appropriate thermal processing enabled a formation of a washcoat that increased the contact area between the catalyst and the support in a DPF.

The thermal conductivity of the tested material is relatively low and decreases monotonically along the temperature from value $\lambda = 2.1$ W $m^{-1}K^{-1}$ w T = 25°C to approx. 1.35 W $m^{-1}K^{-1}$ w T = 600°C mainly due to a drop in thermal diffusivity α. The value of the thermal conductivity for TiO_2 is lower than the value given in literature (approx. 12 $Wm^{-1}K^{-1}$) due to a relatively high porosity of the material. A low thermal conductivity of the material is advantageous for the proposed solution because the heat losses are reduced while heating the filter with the current flow. Thanks to the above it is well substantiated to state that it will not be necessary to use an additional external thermal insulation of the filter.

The performance of the heat exchanger system built forms the basis for continuing the process of design optimization. The designed model heat exchanger allowed the recuperation of 0.4 to 4.2 kW of power at the engine operation parameters used. The coolant temperature on inlet was 17-20°C. If the coolant from the engine cooling system was used on the cooler inlets, the difference in inlet and outlet coolant temperature would be much smaller.

Nomenclature/*Skróty i oznaczenia*

CCRT catalytic continuous regeneration trap/*układ reaktora katalitycznego utleniającego i pokrytego katalitycznie filtra cząstek stałych o ciągłej regeneracji*
CRT continuous regeneration trap/*układ reaktora katalitycznego utleniającego i filtra cząstek stałych o ciągłej regeneracji*
CSF catalyst soot filter/*pokryty katalitycznie filtr cząstek stałych*
DOC diesel oxidation catalyst/*utleniający reaktor katalityczny*
DPF diesel particulate filter/*filtr cząstek stałych*
DPNR diesel particulate NOx reduction/*układ filtra cząstek stałych i absorbera NOx*
PM particulate matter/*cząstka stała*
SiC silicon carbon/*węglik krzemu*

Mr Paweł Fuć, DEng. – doctor in the Faculty of Working Machines and Transportations at Poznań University of Technology.

Dr inż. Paweł Fuć – adiunkt na Wydziale Maszy Roboczych i Transportu Politechniki Poznańskiej.

Bibliography/*Literatura*

[1] Fuć P.: Examination of effectivity of the CRT-DPF based on Ti4O7: WFC10 Congress Proceedings. - 2008, Volume III, 10, s. 474-478: 10th World Filtration Congress, Leipzig, April 14-18.2008.
[2] Fuć P.: Non Pt Catalyst Group in Active Part of New PM Filter Dokument elektroniczny W: 2008 SAE International Powertrains, Fuels and Lubricants Congress, 2008. - 2008-01-1551: CD-ROM. 2008.
[3] Görsmann C.: Catalytic coatings for regeneration (of diesel particulate filters). Haus der Technik Congress: DPF Retrofit of Diesel Engines, Munich, 27.-28.06.2007.
[4] Haralampous O. A., Koltsakis G. C. and Samaras Z. C., Vogt C.-D. and Ohara E., Watanabe Y., Mizutani T.: Reaction and Diffusion Phenomena in Catalyzed Diesel Particulate Filters. Diesel Exhaust Emission Control Modeling (SP-1861) SAE 2004-01-0696.
[5] Heeb N., The importance of secondary pollutants Haus der Technik Congress: DPF Retrofit of Diesel Engines, Munich, 27.-28.06.2007.
[6] Karin P, Hanamura K.: Particulate Matter Trapping and Oxidation on a Catalyst Membrane. 2010 SAE International. Paper 2010-01-0808.
[7] Kyeong O. Lee, Seung Yeon Yang: Parametric Examination of Filtration Processes in Diesel Particulate Filter Membranes with Channel Structure Modification. 2010 SAE International. Paper 2010-01-0537.
[8] Lanzerath P., Traebert A., Massner A., Gaertner U.: Daimler AGInvestigations on Chemical Ageing of Diesel Oxidation Catalysts and Coated Diesel Particulate Filters.. Paper 2010-01-1212.
[9] Maus W., Hodgson J., Vorsmann Ch., Brück R.: PM-Metalit Advanced – the Innovative Particulate Filter for Nanoparticle Reduction. Internationales Wiener Motorensymposium 2010.
[10] Mayer A.,Typische Schadensfälle und ihre Ursachen. Seminar Partikelfilter-Nachrüstung von Dieselmotoren. HdT, 27-28 Juni 2007, München.
[11] Merkisz J., Fuć P.: High porosity sinters TiO2-xNx as an active carrier used in DPF filter: WFC10 Congress Proceedings. - 2008, Volume III, 10, s. 479-483: 10th World Filtration Congress, Lepzig, April 14-18.2008.
[12] Sappok A., Rodriguez R., Wong V.: Characteristics and Effects of Lubricant Chemistry on Ash Properties Impacting Particulate Filter Service Life. -01-1213.
[13] Wojciechowski K., Schmidt M., Zybała R., Merkisz J., Fuć P., Lijewski P.: Comparison of waste heat recovery from the exhaust of a spark ignition and a diesel engine. Journal of Electronic Materials. - 2010, No. 9, s. 2034-2038.
[14] Yan Shu, Romzek M., Lakshmikanth G.: Thermal Analysis of Diesel After-Treatment System. Paper 2010-01-1215.